This article was downloaded by: [Siauliu University Library]
On: 17 February 2013, At: 00:29
Publisher: Taylor & Francis
Informa Ltd Registered in England and Wales Registered Number: 1072954 Registered office: Mortimer House, 37-41 Mortimer Street, London W1T 3JH, UK

Molecular Crystals and Liquid Crystals
Publication details, including instructions for authors and subscription information:
http://www.tandfonline.com/loi/gmcl20

Tunable Nonlinearity in Nematicon Physics

Alessandro Alberucci [a], Armando Piccardi [a] & Gaetano Assanto [a]
[a] NooEL, Nonlinear Optics and OptoElectronics Lab, University "Roma Tre", Via della Vasca Navale 84, Rome, Italy
Version of record first published: 18 Apr 2012.

To cite this article: Alessandro Alberucci , Armando Piccardi & Gaetano Assanto (2012): Tunable Nonlinearity in Nematicon Physics, Molecular Crystals and Liquid Crystals, 558:1, 2-11

To link to this article: http://dx.doi.org/10.1080/15421406.2011.652842

PLEASE SCROLL DOWN FOR ARTICLE

Full terms and conditions of use: http://www.tandfonline.com/page/terms-and-conditions

This article may be used for research, teaching, and private study purposes. Any substantial or systematic reproduction, redistribution, reselling, loan, sub-licensing, systematic supply, or distribution in any form to anyone is expressly forbidden.

The publisher does not give any warranty express or implied or make any representation that the contents will be complete or accurate or up to date. The accuracy of any instructions, formulae, and drug doses should be independently verified with primary sources. The publisher shall not be liable for any loss, actions, claims, proceedings, demand, or costs or damages whatsoever or howsoever caused arising directly or indirectly in connection with or arising out of the use of this material.

Mol. Cryst. Liq. Cryst., Vol. 558: pp. 2–11, 2012
Copyright © Taylor & Francis Group, LLC
ISSN: 1542-1406 print/1563-5287 online
DOI: 10.1080/15421406.2011.652842

Taylor & Francis
Taylor & Francis Group

Tunable Nonlinearity in Nematicon Physics

ALESSANDRO ALBERUCCI,* ARMANDO PICCARDI, AND GAETANO ASSANTO

NooEL, Nonlinear Optics and OptoElectronics Lab, University "Roma Tre", Via della Vasca Navale 84, Rome – Italy

We investigate light self-confinement in nematic liquid crystals with homogeneous planar distribution of the molecular director. Using comb-patterned electrodes we are able to vary the initial orientation, exploiting different degrees of nonlinearity by the electro-optic effect. We experimentally demonstrate tuning of the nonlinearity by studying both single nematicon propagation and planar interactions between two nematicons.

Keywords Liquid Crystals; nonlinear optics; reorientational response; spatial solitons routing; spatial solitons

Downloaded by [Siauliu University Library] at 00:29 17 February 2013

1. Introduction

Nonlinear optics deals with those dielectric properties which depend on the flow of photons (i.e., the light intensity or the power) through them [1]. Every optical medium, however, exhibits a nonlinear response when excited with large enough light intensities. The nonlinear refractive response is often quantified by the Kerr coefficient n_2, setting a linear dependence between the light intensity I and the perturbation in refractive index caused by light itself [2]. Nonlinear optics in nematic liquid crystals (NLC) has attracted a great deal of attention owing to their huge nonlinearity [3], with (effective) Kerr coefficients several orders of magnitude higher than in other fluids such as CS_2 [4].

In this context, one of the most intriguing nonlinear optical phenomena is the formation of nonlinear wave packets preserving their shape while propagating, known as solitons [5,6]. The simplest solitons are bright and can be classified as temporal or spatial according to the domain where wave evolution takes place [7]. Spatial solitons retain their transverse profile owing to the balance between diffraction-induced spreading and nonlinear (Kerr or Kerr-like) self-focusing [5–7], including the "equivalent" self-focusing provided by a *cascaded* quadratic/parametric response [8–23].

Since the pioneering work of Braun et al. [24], light self-confinement and solitons (commonly called "Nematicons" in NLC [25]) have been largely investigated in NLC, including thermal nonlinear effects and beams propagating in capillaries [26], or in planar waveguides [27], or in thick planar cells with initial molecular orientation determined by an external low-frequency electric field [28,29] in order to prevent the Fréedericksz threshold [4]; later improvements included molecular orientation defined by rubbing at angles

*Address correspondence to Alessandro Alberucci, NooEL, Nonlinear Optics and OptoElectronics Lab, University "Roma Tre", Via della Vasca Navale 84, Rome – Italy. E-mail: alberucc@uniroma3.it

differing from 0° or 90°, i.e. avoiding the Fréedericksz transition and allowing the observation of bias-controlled soliton steering [30]. In these and similar configurations, several experiments have been carried out, including interactions between nematicons [31–38], self-steering [39–41], deflection via external perturbations [42–49]. These functionalities have been used to demonstrate the whole set of all-optical devices [50–53].

In this paper we focus on the dependence of nematicon evolution on the initial properties of the NLC, with particular attention to the role of both nonlinearity and nonlocality [54], the latter relevant even in different contexts [55] but, in the frame of soliton physics, providing stability to two dimensional optical spatial solitons [56]. To carry out this comparison we employ a comb-patterned cell, as described in Ref. 57, which allows changing the effective initial orientation via the applied voltage bias. Our aim hereby is to study and characterize the nonlinear index well formed in NLC by the self-confined beam. To this extent we investigate the role of the nonlinear index profile on the solitary beam itself and on another beam propagating nearby, studying the individual nematicon evolution and the interaction between two nematicons, respectively.

Downloaded by [Siauliu University Library] at 00:29 17 February 2013

2. Theoretical Background

Nematic liquid crystals are a phase of matter featuring a high degree of orientational order at the molecular level, but lacking positional order in the long range [4]. Their physical properties are intermediate between those of liquids and solids, i.e. they flow like a fluid but at the same time exhibit an anisotropic dielectric response typical of solid-state crystals [4]. To describe them it is often sufficient to introduce the density distribution for the orientation of the main (major) molecular axis. Most NLC are macroscopically uniaxial; hence, a single vector (optic axis) fully identifies the average direction of the elongated molecules: it is called molecular director $\hat{n}$ and determines the symmetry of the system on a macroscopic level. The eigenvalues of the permittivity tensor are $\varepsilon_{//}$ and $\varepsilon_{\perp}$ for electric fields polarized parallel and perpendicular to $\hat{n}$, respectively. Each element of the dielectric tensor is given by $\varepsilon_{jk} = \varepsilon_{\perp}\delta_{jk} + \varepsilon_a n_j n_k (j, k = x, y, z)$, being n_j the Cartesian components of the director $\hat{n}$ and having defined the dielectric anisotropy $\varepsilon_a = \varepsilon_{//} - \varepsilon_{\perp}$. The extraordinary refractive index n_e for a plane wave with wave-vector along $\hat{z}$ is $n_e = \sqrt{\varepsilon_{yy} - \varepsilon_{yz}^2/\varepsilon_{zz}}$, whereas the walk-off angle δ can be expressed as $\delta = \arctan(\varepsilon_{yz}/\varepsilon_{zz})$ (Fig. 1(a)); finally, we often use the two refractive indices $n_{\perp} = \sqrt{\varepsilon_{\perp}}$ and $n_{//} = \sqrt{\varepsilon_{//}}$. We underline that the optical anisotropy depends on the width of the director distribution via the order parameter S [4].

Considering a spatial distribution such that the director lies everywhere in the plane yz in the absence of light and assuming an input beam entering the NLC with polarization

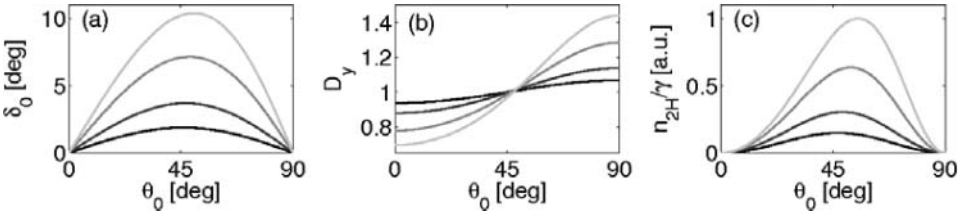

Figure 1. Walk-off angle (a), diffraction coefficient (b) and nonlinear nonlocal Kerr coefficient (c) versus initial orientation θ_0; here $n_{\perp} = 1.5$, with $n_{//}$ equal to 1.55, 1.6, 1.7 and 1.8 from the black line towards the light gray line, respectively.

along y and phase fronts normal to $\hat{z}$, and naming θ the angle formed by director $\hat{n}$ with axis $\hat{z}$, the molecules can only rotate within the plane yz and the electromagnetic wave can be completely described by the magnetic field H_x [58]. Thus, calling K the Frank elastic constant in the single constant approximation, paraxial light propagation in the highly nonlocal limit and for adiabatic variations in $\hat{n}$ is governed by:

$$2ik_0 n_e^{(b)} \left(\frac{\partial A}{\partial z} + \tan \delta^{(b)} \frac{\partial A}{\partial y} \right) + D_y \frac{\partial^2 A}{\partial y^2} + \frac{\partial^2 A}{\partial x^2} + k_0^2 \Delta n_e^2 A = 0, \tag{1}$$

$$\nabla^2 \theta + \gamma \, |A|^2 \sin[2(\theta - \delta^{(b)})] = 0, \tag{2}$$

where $A = H_x e^{-ik_0 n_e^{(b)} z}$ is the slowly varying envelope of the magnetic field, k_0 is the vacuum wave number, $\delta^{(b)}$ and $n_e^{(b)}$ are the walk-off and the refractive index computed at the intensity peak, respectively, $D_y = (n_e^{(b)})^2/\varepsilon_{zz}$ is the diffraction coefficient along y (plotted in Fig. 1(b)), $\gamma = \varepsilon_0 \varepsilon_a \sigma^2/(4K)$ with $\sigma = Z_0/n_e^{(b)} \cos \delta^{(b)}$ (Z_0 is the vacuum impedance) and $\Delta n_e^2 = n_e^2 - (n_e^{(b)})^2$ is the nonlinear increase in refractive index [58]. Equation (1) is an anisotropic nonlinear Schrödinger equation ruling the optical wave evolution, whereas Eq. (2) states the equilibrium between the different torques acting on the molecules [3,4]. The latter equation allows computing the nonlinear perturbation of the quantities in Eq. (1) depending on the dielectric tensor, such as D_y and Δn_e^2 (governing the beam waist for a single-hump input) and $\delta^{(b)}$ (governing the beam trajectory in the absence of gradients in the director field or boundary effects [39]) by using the straightforward relations $n_z = \cos\theta$ and $n_y = \sin\theta$.

Let us now take a homogeneous director distribution with $\theta = \theta_0$ for $A = 0$ and set $\theta = \theta_0 + \psi$, with ψ the all-optical perturbation. For small nonlinear perturbations (i.e., $\psi << \theta_0$), Eq. (2) can be linearized; applying the Green function formalism for its solution yields [58]:

$$\Delta n_e^2 = n_{2H}(\theta_0) \, P g(x, y, z). \tag{3}$$

In Eq. (3) we introduced the nonlocal effective Kerr coefficient:

$$n_{2H}(\theta_0) = 2\gamma n_e^2(\theta_0) \tan \delta_0 \sin[2(\theta_0 - \delta_0)], \tag{4}$$

where $\delta_0 = \delta(\theta_0)$ and $g = \iiint |u|^2 \, G dx dy dz$, with $A = \sqrt{P} u$ and G being the Green function of the assigned geometry. Equation (4) suggests that, in homogeneous samples of NLC, the nonlinearity can be tuned by changing the initial angle θ_0. Moreover, Eq. (4) establishes that, for fixed $\varepsilon_\perp$ and K, n_{2H} depends quadratically on ε_a in the limit of small anisotropies [59]. n_{2H} versus θ_0 is plotted in Fig. 1(c) for various anisotropies (i.e., different NLC mixtures): the maximum nonlinear effects are predicted for θ_0 close to 45° for very small anisotropies, moving towards higher θ_0 as anisotropy increases and going to zero for both $\theta_0 = 0$ (appearance of Fréedericksz threshold) and $\theta_0 = 90°$ (director parallel to the optical electric field).

From Eq. (3) we can infer that the shape of the nonlinear perturbation depends on the geometry via the Green function G. The nonlocality, generally quantified as the ratio between the widths of the nonlinear index well and of the beam intensity profile, will therefore depend only on the boundary conditions to be applied in the specific case. In the highly nonlocal limit (i.e., beam waist approaching zero), the widths of g and G will coincide; hence, the form of Δn_e^2 will depend on the boundary conditions, with a width proportional to the shortest side of the cell. Otherwise stated, shape and size of the cell

Downloaded by [Siauliu University Library] at 00:29 17 February 2013

employed to confine the NLC will determine the shape of the potential Δn_e^2, whereas the anchoring conditions at the interfaces control its size.

These findings hold valid in the perturbative regime, i.e. for small optically-induced variations in the director distribution. In the most general case the highly nonlocality of the system guarantees that the shape of ψ remains unaltered, the largest difference consisting in a saturating relationship between the peak of ψ and the power P, due to the orientational nature of the nonlinearity [58,60].

3. Description of the Sample

Figures 2(a–b) show the sketch of the cell employed in the experiments. The NLC is contained between two glass slides parallel to the plane yz, separated by spacers of thickness $L = 100\,\mu$m. On each slide two interdigitated comb electrodes are realized in Indium Tin Oxide, with periodicity along z; fingers belonging to the same electrode have a period $2\,\Lambda = 60\,\mu$m and fingers of different electrodes a minimum distance $\Lambda/2 = 15\,\mu$m. When an electric potential V is externally applied between the two electrodes, the NLC molecules are subject to an electric field E_{LF} periodic along z with period $2\,\Lambda$. NLC are actually sensitive to the square modulus of E_{LF} (see Eq. (2)) [3,4], therefore the effective periodicity is Λ. Moreover, the E_{LF} field lines accumulate close to the interfaces, with direction almost parallel to the z axis due to the smallness of $\Lambda/2$ in comparison with L (see Fig. 2(b)). Since the width of the Green function in a planar cell is comparable to L, the periodic perturbation close to the interfaces is flattened by the NLC response, with director reorientation diffusing towards the cell centre due to the intermolecular (elastic) links.

We can neglect E_{LF} along $\hat{x}$ due to $\Lambda \ll L$; thus, we consider only the component of E_{LF} along $\hat{z}$, the latter being zero to first approximation and equal to $2\mathrm{V}/\Lambda$ underneath and

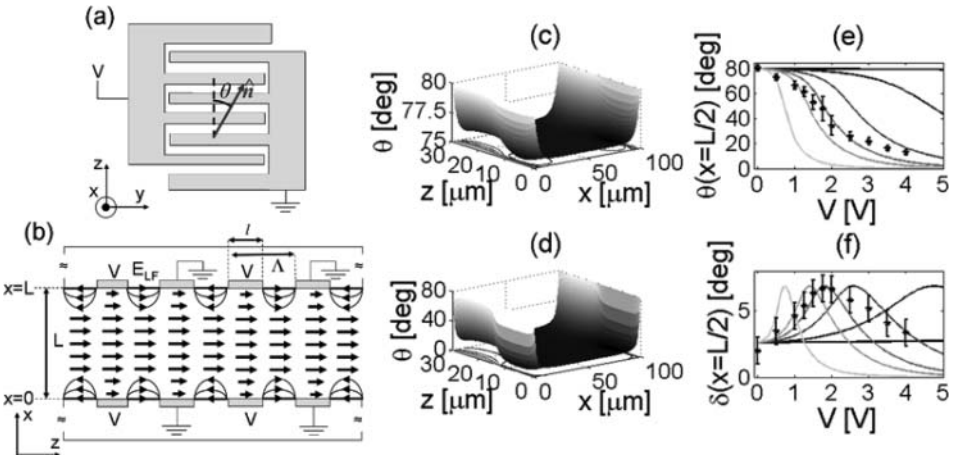

Figure 2. Top (a) and side (b) sketches of the comb-patterned cell. In (b) the solid lines with arrows indicate qualitatively the low frequency electric field E_{LF}, whereas the arrows refer to the spatial distribution of the director $\hat{n}$. Reorientation in the plane xz for V = 1 V (c) and V = 5 V (d), with $\kappa = 1.3 \times 10^5\ \mathrm{m}^{-1}$; the initial rubbing angle θ_R is set to 80°. Reorientation angle in the cell mid-plane (e) and soliton walk-off (f) versus applied bias V for $\kappa = 5 \times 10^4, 2 \times 10^5, 1.3 \times 10^5, 2 \times 10^5, 4 \times 10^5, 2 \times 10^6\ \mathrm{m}^{-1}$ (solid lines) and the measured data (points with error bars). In (e–f) κ increasing from left to right. In the simulations we used $K = 12 \times 10^{-12}$ Nm and $\varepsilon_{LF} = 14$.

Downloaded by [Siauliu University Library] at 00:29 17 February 2013

between the electrodes, respectively, with an exponential decay towards the cell mid-plane (that is, going as $e^{-\kappa x}$ at the bottom interface). Such hypotheses imply a planar reorientation for $\hat{n}$: the cell is tunable with bias and behaves as a planar sample with anchoring angle (initial director orientation) determined by the applied voltage V.

Having defined $\gamma_{LF} = \varepsilon_0 \varepsilon_{LF}/(2K)$, the director distribution can be computed by solving the equation $\partial^2\theta/\partial x^2 + \partial^2\theta/\partial z^2 - \gamma_{LF}|E_{LF}|^2 \sin(2\theta) = 0$ with boundary conditions $\theta(x = 0) = \theta(x = L) = \theta_R$ fixed by the rubbing on the interfaces [4,28,58]. Given the periodicity, it is sufficient to solve the latter equation in one period. Figure 2(c–d) shows the bias-induced director distribution for two applied voltages: as predicted, around the cell mid-plane θ is flat, i.e. the director is homogeneously distributed as in a standard planar cell, but with an effective initial orientation θ_0 given by $\theta(x = L/2)$; the behaviour versus applied bias V is graphed in Fig. 2(e) for several κ. Figure 2(f) plots the soliton walk-off corresponding to Fig. 2(e) together with data from the experimental measurements: the direct comparison demonstrates a the best-fit for $\kappa = 2 \times 10^5\ \mathrm{m}^{-1}$, with discrepancies increasing with L owing to the appearance of vertical electric field components, neglected in our simplified model.

4. Single Nematicon Propagation

Using the cell described above we explored the tunability of the NLC nonlinear response by investigating single nematicon propagation for various initial angles θ_0, tuned by the bias V (Fig. 2). The chosen NLC was the commercial mixture E7, featuring $n_\perp = 1.5$ and $n_{//} = 1.7$ in the near infrared. We injected a TEM_{00} beam of wavelength 1064 nm with waist of about 5 μm, polarized along $\hat{y}$ in order to couple to the extraordinary component inside the sample. The intensity distribution inside the cell was acquired by imaging the photons scattered along $\hat{x}$ with a CCD camera [28].

Examples of measured beam evolution are presented in Fig. 3. In this range of powers, the beams propagate at the linear walk-off δ_0 with $\hat{z}$ (see Fig. 2(f) for walk-off versus applied bias) [40]. Figure 4 graphs the beam waist versus power: at low powers the beam diffracts, with divergence depending on V via D_y. As power increases, the beam undergoes self-focusing (waists versus z reduce with respect to the linear case), up to self-confinement

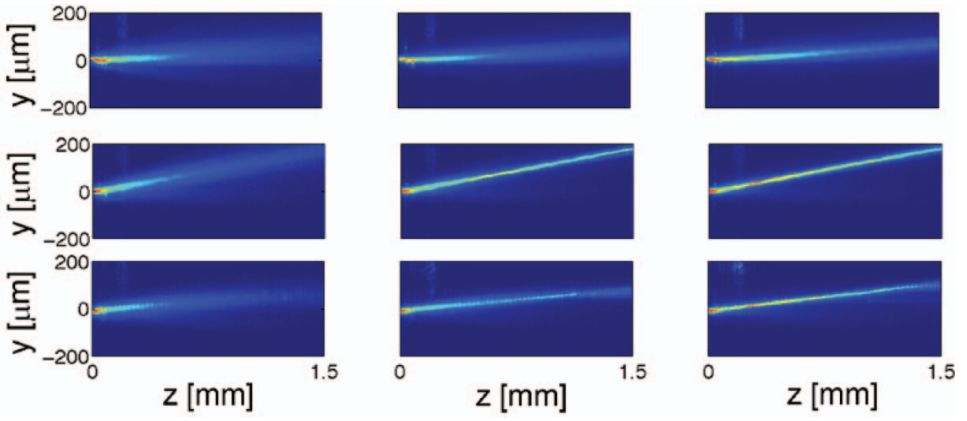

Figure 3. Acquired beam evolution in the plane yz. Beam powers are 1, 4, 10 mW from left to right, respectively, and voltages V = 0, 1.75, 4 V from top to bottom, respectively.

Downloaded by [Siauliu University Library] at 00:29 17 February 2013

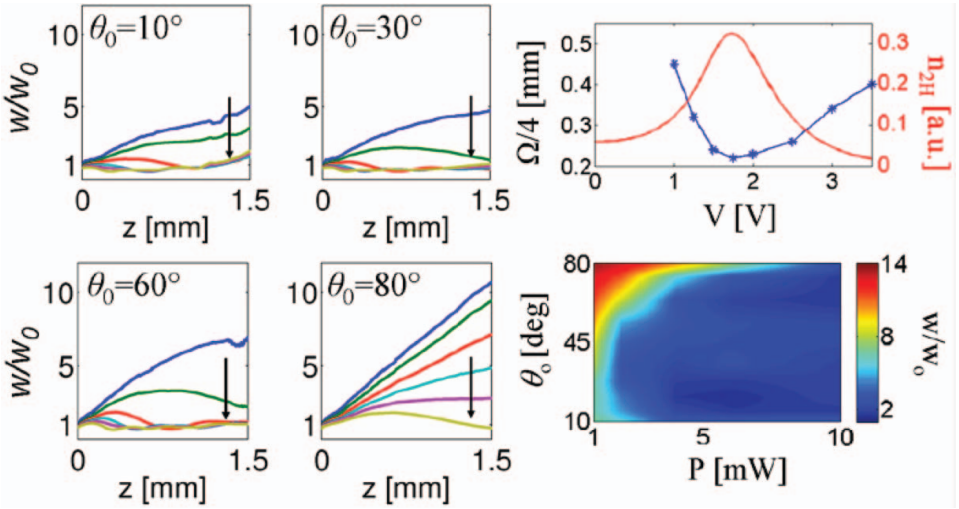

Figure 4. Leftmost columns: nematicon waist versus z for four initial orientations θ_0; lines correspond to P = 1, 2, 4, 6, 8, 10 mW from top to bottom, respectively. The waist is normalized to the input value w_0. Right column: on the top, plot of the measured breathing period Ω (points) and nonlinearity n_{2H} (solid line) versus applied voltage V; on the bottom, plot of the z-averaged normalized waist versus beam power P and initial orientation θ_0.

(a single-hump beam is self-confined when its waist is bound along z). Consistently with Eq. (4) (see Fig. 1(c)), the self-focusing is maximum for $\theta_0 \cong \pi/4$ (i.e., V = 1.75 V), decreases both for θ_0 larger and smaller than $\pi/4$ (i.e., V = 0 and 4 V, respectively). The behaviour between $\pi/4 - \Theta$ and $\pi/4 + \Theta$ ($0 < \Theta < \pi/4$) at high powers differs from the perturbative regime: in fact, for $\pi/4 < \theta_0 < \pi/2$ saturation of reorientation becomes relevant and reduces the observed nonlinear effects with respect to the case $0 < \theta_0 < \pi/4$ (see the cases $\theta_0 = 10^\circ$ and $\theta_0 = 80^\circ$ in Fig. 4).

In the highly nonlocal limit, the nonlinear potential Δn_e^2 can be approximated with a parabolic profile [61,62]; hence, self-confined beams should exhibit a waist sinusoidally oscillating in propagation, with a period Ω proportional to the inverse of the square root of $n_{2H}P$. In actual facts, the waist differs from the sinusoidal shape owing to the unavoidable scattering losses. Clearly, the latter also inhibit the observation of rigorously shape-preserving wave packets.

To compare the measured data on versus θ_0 with the theoretical predictions for n_{2H}, we graph the distance from the input where first relative maximum in waist occurs (Fig. 4): in agreement with predictions, the shortest period is obtained for V = 1.75 V, corresponding to $\theta_0 = \pi/4$. The last panel of Fig. 4 shows the averaged waist $\bar{w}$ along z (defined as $\bar{w} = (1/z_0)\int_0^{z_0} w(z)dz$) versus nematicon power P and θ_0: in agreement with the previous data, maximum self-trapping takes place for $\theta_0 = \pi/4$.

5. Nematicon-Nematicon Interactions

Having addressed the propagation of a single nematicon, here we focus on the interaction between two self-confined beams and its dependence on the initial angle θ_0. This is another approach towards validating the variation in nonlinearity: we expect that the two solitons attract each other via the nonlinear index perturbation due to each beam, oscillating around

Downloaded by [Siauliu University Library] at 00:29 17 February 2013

one another with a period decreasing with the excitation $n_{2H}P$. Owing to the high nonlocality, we expect long range interactions, with non-negligible interactions for mutual distances of the size of L; hence, experiments with two nematicons can be employed to test the shape of the nonlinear perturbation Δn_e^2, i.e., the nonlocality. Moreover, high nonlocality implies an always attractive potential between solitons not overlapping in the input section, at variance with pure Kerr media where the repulsive or attractive character of the interaction depends on the beam relative phase [5,7].

To perform the experiments we split a TEM_{00} beam into two, each carrying the same power. The two beams impinge on the sample with the same phase. At the cell input the separation d between the two beams was varied in order to study how it affects propagation. The launching conditions were controlled so that both wave vectors were parallel to $\hat{z}$.

Typical experimental results are shown in Fig. 5. If distance d and power P of each soliton are fixed, the interaction strength follows the theoretical curve of n_{2H} (Fig. 1(c)), as demonstrated by the z-position of the first crossing versus applied voltage V (Fig. 6(a)) (clearly, stronger interactions imply a first crossing closer to the input). Moreover, experiments for $d \geq L$ show that nematicons do not appreciably interact for any available power (the latter limited by the insurgence of time-dependent instabilities), independently from the applied bias, thus confirming that the width of the nonlinear index well induced by a single nematicon is approximately L [38,63]. Figure 6(b) plots the first crossing versus initial distance in correspondence to the maximum nonlinearity: as predictable, nematicons cross each other at shorter z when they are launched closer, with attraction increasing with power. The first nematicon crossing for d larger than 80μm increases abruptly, confirming that Δn_e^2 is fixed by L. In the experiments discussed hereby the minimum investigated d was 20 μm, so that the input beams did not significantly overlap. Some results in the highly

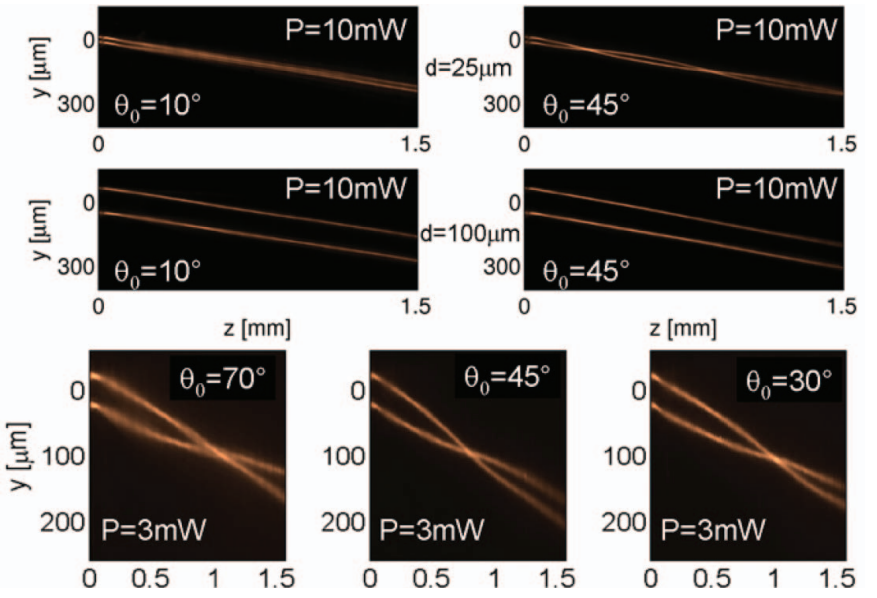

Figure 5. Top: nematicon propagation in yz at power P = 10 mW initial distance $d = 25$ μm but different θ_0. Middle: same as above but $d = 100$ μm. Bottom: nematicon interaction at fixed power P = 3 mW and initial distance $d = 45$ μm, for three orientations of θ_0.

Downloaded by [Siauliu University Library] at 00:29 17 February 2013

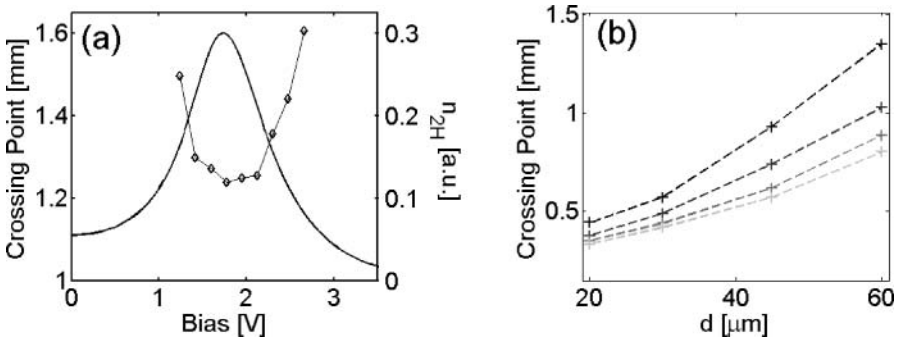

Figure 6. (a) First crossing (points) and nonlinear coefficient n_{2H} versus applied voltage; experiments were carried out for $d = 45$ μm and P = 3 mW. (b) First crossing (points connected by dashed lines) versus initial separation d for V = 1.8 V; the lines correspond to P = 4, 6, 8, 10 mW. from top to bottom, respectively.

nonlocal limit can be found in Ref. 64. Finally, the shape of the curve follows the theoretical predictions, see Ref. 38.

6. Conclusions

We investigated beam self-trapping in homogeneous NLC samples and its dependence on the initial orientation of the molecules. We showed that the nonlinearity, i.e. the magnitude of the all optical change in refractive index, depends on the direction of the optic axis in the absence of light, whereas the nonlocality, i.e. the width of the nonlinear index well, depends on the cell geometry. We experimentally verified such results using a cell with comb-patterned electrodes, and effective anchoring conditions depending on the voltage. We studied single nematicon propagation and interactions between two nematicons, the experimental results confirming the theoretical predictions.

Acknowledgments

We are grateful to Marco Peccianti, Malgosia Kaczmarek and Michal Kwasny for various contributions to this study. A.A. thanks "Regione Lazio" for financial support. Effort partially sponsored by the Air Force Office of Scientific Research, Air Force Material Command, USAF, under grant number FA-8655-10-1-3010. The U.S. Government is authorized to reproduce and distribute reprints for Governmental purpose notwithstanding any copyright notation thereon.

References

[1] Shen, Y. R. (1984). *The Principles of Nonlinear Optics*, Wiley: New York.
[2] Chiao, R. Y., Garmire, E., & Townes, C. H. (1964). *Phys. Rev. Lett.*, *13*, 479–482.
[3] Zeldovich, B., Pilipetskii, N., Sukhov, A., & Tabiryan, N. (1980). *JETP Letters*, *31*, 263–269.
[4] Khoo, I. C. (2009). *Phys. Rep.*, *471*, 221–267.
[5] Stegeman, G. I., & Segev, M. (1999). *Science*, *286*, 1518–1523.
[6] Conti, C., & Assanto, G. (2004) "Nonlinear Optics Applications: Bright Spatial Solitons", In: R. D. Guenther, D. G. Steel, & L. Bayvel (Eds.), *Encyclopedia of Modern Optics*, 5, 43–55, Elsevier: Oxford.

Downloaded by [Siauliu University Library] at 00:29 17 February 2013

[7] Kivshar, Y. R., & Agrawal, G. P. (2003). *Optical Solitons*, Academic: San Diego.
[8] Torruellas, W. E., Wang, Z., Hagan, D. J., Van Stryland, E. W., Stegeman, G. I., Torner, L., & Menyuk, C. R. (1995). *Phys. Rev. Lett.*, *74*, 5036.
[9] Schiek, R., Baek, Y., & Stegeman, G. I. (1996). *Phys. Rev. E*, *53*, 1138–1141.
[10] Torruellas, W. E., Assanto, G., Lawrence, B. L., Fuerst, R. A., & Stegeman, G. I. (1996). *Appl. Phys. Lett.*, *68*, 1449–1451.
[11] Leo, G., Assanto, G., & Torruellas, W. E. (1997). *Opt. Lett.*, *22*, 7–9.
[12] Leo, G., Assanto, G., & Torruellas, W. E. (1997). *J. Opt. Soc. Am. B*, *14*, 3134–3142.
[13] Costantini, B., De Angelis, C., Barthelemy, A., Laureti Palma, A., & Assanto, G. (1997). *Opt. Lett.*, *22*, 1376–1378.
[14] Leo, G., & Assanto, G. (1997). *Opt. Lett.*, *22*, 1391–1393.
[15] Torner, L., Menyuk, C. R., & Stegeman, G. I. (1995). *J. Opt. Soc. Am. B*, *12*, 889–897.
[16] Canva, M. T. G., Fuerst, R. A., Baboiu, S., Stegeman, G. I., & Assanto, G. (1997). *Opt. Lett.*, *22*, 1683–1685.
[17] De Rossi, A., Assanto, G., Trillo, S., & Torruellas, W. E. (1998). *Opt. Commun.*, *150*, 390–398.
[18] Assanto, G., Conti, C., Leo, G., Stegeman, G. I., Torruellas, W. E., & Trillo, S. (1998). *J. Nonl. Opt. Phys. Mat.*, *7*, 345–368.
[19] Fuerst, R. A., Canva, M. T.G., Stegeman, G. I., Leo, G., & Assanto, G. (1998). *Opt. & Quantum Electron.*, *30*, 907–921.
[20] Buryak, A. V., Di Trapani, P., Skryabin, D. V., & Trillo, S. (2002). *Phys. Rep.*, *370*, 73–235.
[21] Assanto, G., & Stegeman, G. I. (2002). *Opt. Express*, *10*, 388–396.
[22] Leo, G., Colace, L., Amoroso, A., Di Falco, A., & Assanto, G. (2003). *Opt. Lett.*, *28*, 1031–1033.
[23] Leo, G., Amoroso, A., Colace, L., Assanto, G., Roussev, R. V., & Fejer, M. M. (2004). *Opt. Lett.*, *29*, 1778–1780.
[24] Braun, E., Faucheux, L. P., & Libchaber, A. (1993). *Phys. Rev. A*, *48*, 611–622.
[25] Assanto, G., & Karpierz, M. (2009). *Liq. Cryst.*, *36*, 1161–1172.
[26] Warenghem, M., Henninot, J. F., & Abbate, G. (1998). *Mol. Cryst. Liq. Cryst.*, *320*, 207–230.
[27] Karpierz, M., Sierakowski, M., Swillo, M., & Wolinski, T. (1998). *Mol. Cryst. Liq. Cryst.*, *320*, 157–163.
[28] Peccianti, M., Assanto, G., De Luca, A., Umeton, C., & Khoo, I. C. (2000). *Appl. Phys. Lett.*, *77*, 7–9.
[29] Peccianti, M., & Assanto, G. (2002). *Phys. Rev. E.*, *65*, 035603.
[30] Peccianti, M., Conti, C., Assanto, G., De Luca, A., & Umeton, C. (2004). *Nature*, *432*, 733–737.
[31] Peccianti, M., Brzdiekwicz, K., & Assanto, G. (2002). *Opt. Lett.*, *27*, 1460–1462.
[32] Hu, W., Zhang, T., Guo, Q., Xuan, L., & Lan, S. (2006). *Appl. Phys. Lett.*, *89*, 071111.
[33] Fratalocchi, A., Piccardi, A., Peccianti, M. & Assanto, G. (2007). *Opt. Lett.*, *32*, 1447–1449.
[34] Alberucci, A., Peccianti, M., Assanto, G., Dyadyusha, A., & Kackmarek, M. (2006). *Phys. Rev. Lett.*, *97*, 153903.
[35] Fratalocchi, A., Piccardi, A., Peccianti, M., & Assanto, G. (2007). *Phys. Rev. A*, *75*, 063835.
[36] Skuse, B. D., & Smyth, N. F. (2009). *Phys. Rev. A*, *79*, 063806.
[37] Izdebskaya, Y. V., Shvedov, V. G., Desyatnikov, A. S., Krolikowski, W., Belic, M., Assanto, G., & Kivshar, Y. S. (2010). *Opt. Express*, *18*, 3258–3263.
[38] Kwasny, M., Piccardi, A., Alberucci, A., Peccianti, M., Kaczmarek, M., Karpierz, M., & Assanto, G. (2011). *Opt. Lett.*, *36*, 2566–2568.
[39] Alberucci, A., Peccianti, M., & Assanto, G. (2007). *Opt. Lett.*, *32*, 2795–2797.
[40] Piccardi, A., Alberucci, A., & Assanto, G. (2010). *Appl. Phys. Lett.*, *96*, 061105.
[41] Piccardi, A., Alberucci, A., & Assanto, G. (2010). *Phys. Rev. Lett.*, *104*, 213904.
[42] Pasquazi, A., Alberucci, A., Peccianti, M., & Assanto, G. (2005). *Appl. Phys. Lett.*, *87*, 261104.
[43] Peccianti, M., Assanto, G., Dyadyusha, S., & Kaczmarek, M. (2007). *Phys. Rev. Lett.*, *98*, 113902.
[44] Peccianti, M., Dyadyusha, S., Kaczmarek, M., & Assanto, G. (2008). *Phys. Rev. Lett.*, *101*, 153902.
[45] Piccardi, A., Assanto, G., Lucchetti, L., & Simoni, F. (2008). *Appl. Phys. Lett.*, *93*, 171104.

Downloaded by [Siauliu University Library] at 00:29 17 February 2013

[46] Izdebskaya, Y. V., Shvedov, V. G., Desyatnikov, A. S., Krolikowski, W., & Kivshar, Y. S. (2010). *Opt. Lett.*, *35*, 1692–1694.
[47] Assanto, G., Skuse, B. D., & Smyth, N. F. (2010). *Phys. Rev. A*, *81*, 063811.
[48] Beeckman, J., Neyts, K., & Haelterman, M. (2006). *J. Opt. A: Pure Appl. Opt.*, *8*, 214–220.
[49] Barboza, R., Alberucci A., & Assanto, G. (2011). *Opt. Lett.*, *36*, 2725–2727.
[50] Peccianti, M., Conti, C., Assanto, G., De Luca, A., & Umeton, C. (2002). *Appl. Phys. Lett.*, *81*, 3335–3337.
[51] Serak, S. V., Tabiryan, N. V., Peccianti, M., & Assanto, G. (2006). *IEEE Photon. Techn. Lett.*, *18*, 1287–1289.
[52] Assanto, G., & Peccianti, M. (2007). *J. Nonl. Opt. Phys. Mat.*, *16*, 37–48.
[53] Piccardi, A., Alberucci, A., Bortolozzo, U., Residori, S., & Assanto, G. (2010). *IEEE Photon. Techn. Lett.*, *22*, 694–696.
[54] Peccianti, M., Conti, C., & Assanto, G. (2005). *Opt. Lett.*, *30*, 415–417.
[55] Vitrant, G., Reinisch, R., Paumier, J. Cl., Assanto, G., & Stegeman, G. I. (1989). *Opt. Lett.*, *14*, 898–890.
[56] Conti, C., Peccianti, M., & Assanto, G. (2003). *Phys. Rev. Lett.*, *91*, 073901.
[57] Piccardi, A., Peccianti, M., Assanto, G., Dyadyusha, A., & Kaczmarek, M. (2009). *Appl. Phys. Lett.*, *94*, 091106.
[58] Alberucci, A., Piccardi, A., Peccianti, M., Kaczmarek, M., & Assanto, G. (2010). *Phys. Rev. A*, *82*, 023806.
[59] Piccardi, A., Trotta, M., Kwasny, M., Alberucci, A., Asquini, R., Karpierz, M., D'Alessandro, A., & Assanto, G. (2011). *Appl. Phys. B*, *104*, 805–811.
[60] Alberucci, A., & Assanto, G. (2010). *Opt. Lett.*, *35*, 2520–2522.
[61] Snyder, A. W., & Mitchell, D. J. (1997). *Science*, *276*, 1538–1541.
[62] Conti, C., Peccianti, M., & Assanto, G. (2004). *Phys. Rev. Lett.*, *92*, 113902.
[63] Rotschild, C., Alfassi, O., Cohen, O., & Segev, M. (2006). *Nature Phys.*, *2*, 769–774.
[64] Hu, W., Ouyang, S., Yang, P., Guo, Q., & Lan, S. (2008). *Phys. Rev. A*, *77*, 033842.

Downloaded by [Siauliu University Library] at 00:29 17 February 2013